**Article:**

He, Y., Xiong, W., Hu, P. et al. (10 more authors) (2024) Climate change enhances stability of wheat-flowering-date. Science of The Total Environment, 917. 170305. ISSN 0048-9697

https://doi.org/10.1016/j.scitotenv.2024.170305

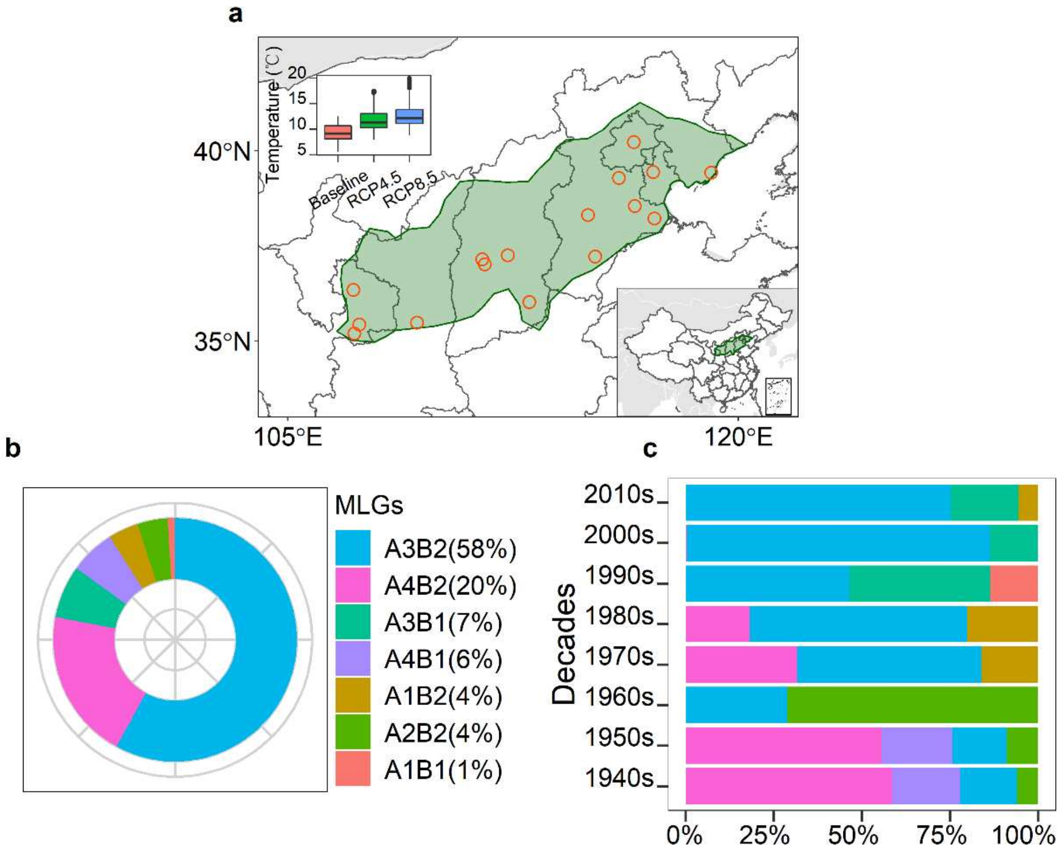


**Figure 1. Study area, climate change, and genetic diversity. a**, Map of the 16 locations of the Northern China Winter Wheat Region (NCWWR), where this study was conducted (light green area); Target mean air temperature of wheat growing season under baseline (1981–2010) and RCP4.5 and RCP8.5 projected climates (2036–2065). Boxes in **a** show the median, an upper and lower hinge corresponding to the 25$^{th}$ and 75$^{th}$ percentiles of the distribution (first and third quartiles) and the whiskers, which show data dispersion up to 1.5 times the inter-quantile range; filled black circles are outliers. **b**, Multi-locus genotypes (MLGs) identified among 100 adapted wheat varieties and landraces. The photoperiod and vernalization loci were combined to construct haplotypes in which A1 (*Ppd-A1a*+*Ppd-D1a*), A2 (*Ppd-A1a*+*Ppd-D1b*), A3 (*Ppd-A1b*+*Ppd-D1a*), and A4 (*Ppd-A1b*+*Ppd-D1b*) in which the a and b alleles represent different photoperiod insensitivity and sensitivity, respectively. While B1 (*Vrn-D1*) and B2 (*vrn-D1*) represent the spring and winter vernalization alleles, respectively. See Supplementary Table 1 for details. **c**, Era-wise distribution of release of the MLGs. Note: 1940s represents the varieties dating during and prior to the 1940s. The inset in 1a shows the Nanhai zhudao.

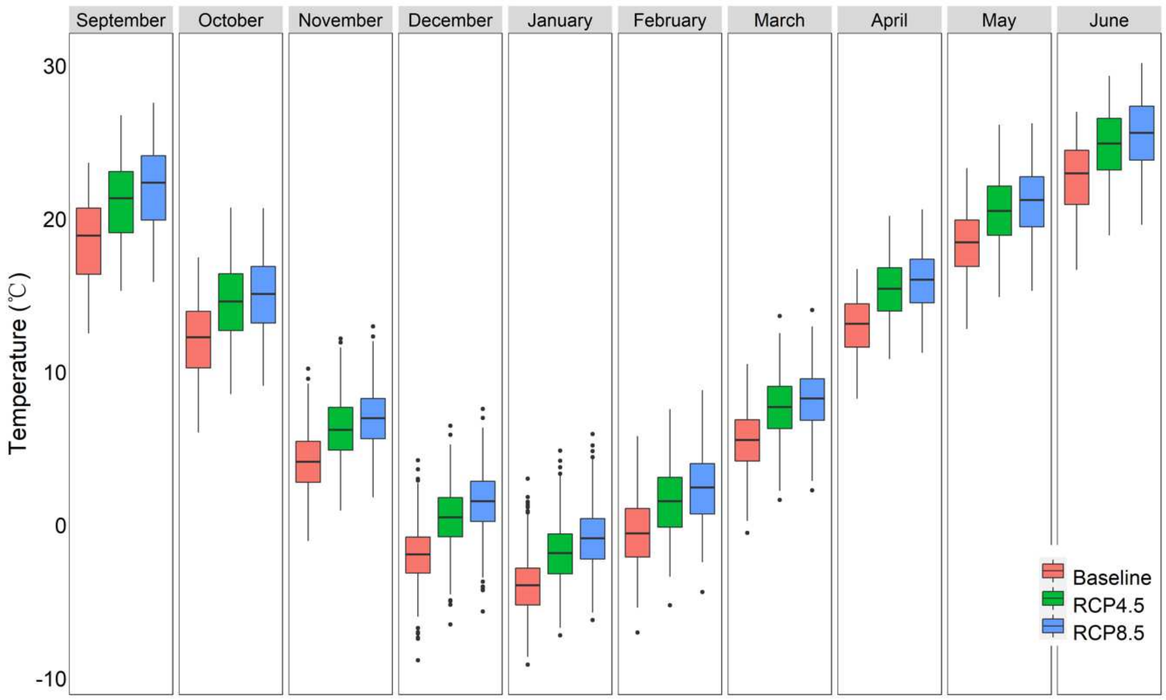


**Figure 2. Distribution of mean monthly air temperature of wheat growing-season at 16 locations of the Northern China Winter Wheat Region (NCWWR) under baseline (1981–2010), RCP4.5 and RCP8.5 projected climates (2036–2065) of the 16 locations of the Northern China Winter Wheat Region (NCWWR).** Boxes show the median, an upper and lower hinge corresponding to the 25th and 75th percentiles of the distribution (first and third quartiles) and the whiskers, which show data dispersion up to 1.5 times the inter-quantile range; filled black circles are outliers.

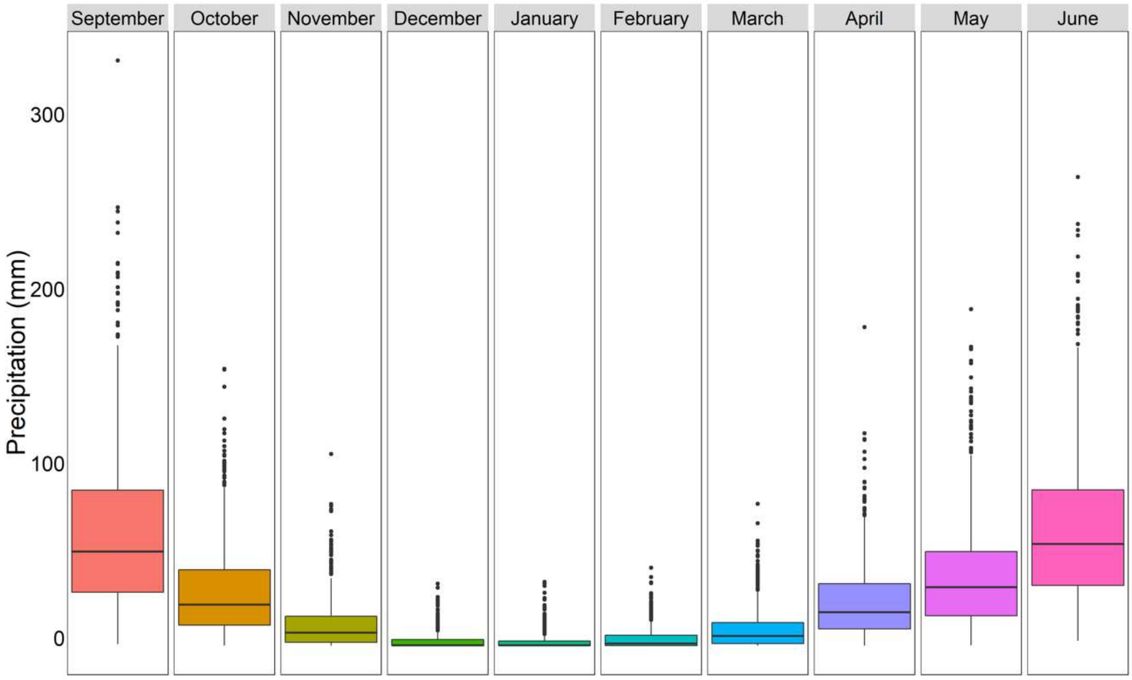


**Figure 3. Distribution of monthly accumulated precipitation of growing-season at 16 locations of the Northern China Winter Wheat Region (NCWWR) for the period 1961–2015.** Boxes show the median, an upper and lower hinge corresponding to the 25$^{th}$ and 75$^{th}$ percentiles of the distribution (first and third quartiles) and the whiskers, which show data dispersion up to 1.5 times the inter-quantile range; filled black circles are outliers.

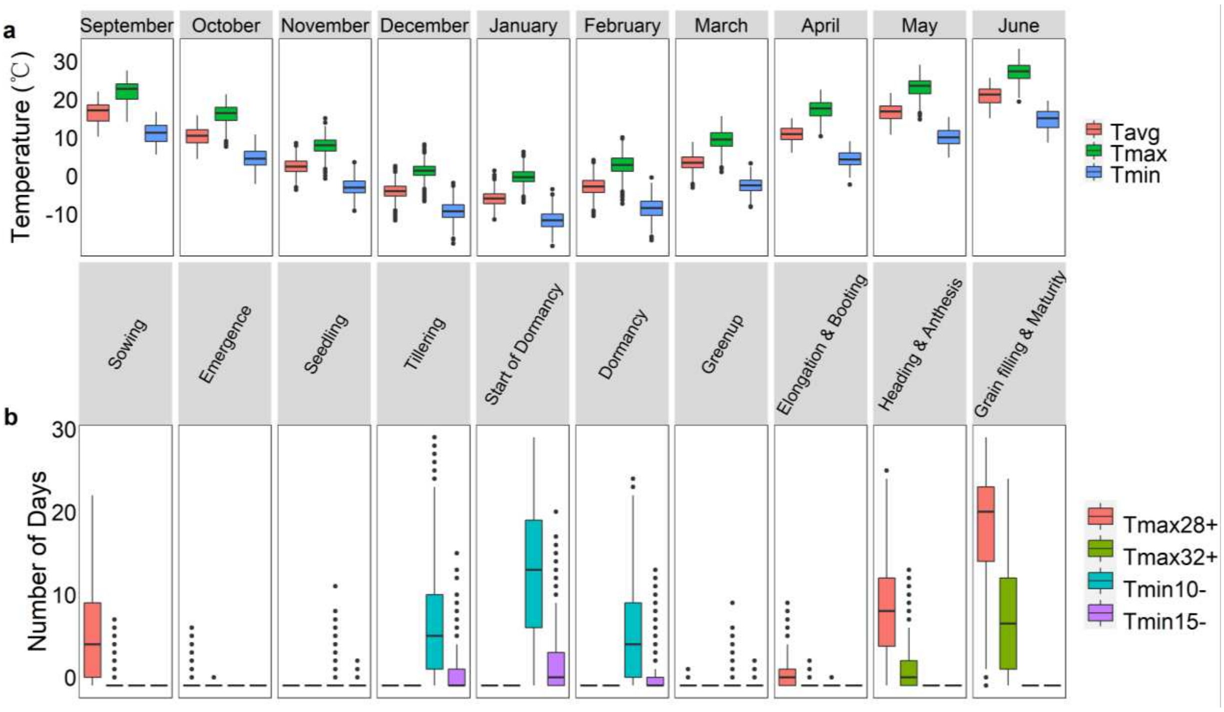


**Figure4. Variation in monthly air temperature of growing-season at 16 locations of the Northern China Winter Wheat Region (NCWWR) for the period 1961–2015.** **a**, Boxplot of averaged monthly temperature (Tavg), maximum temperature (Tmax), and minimum temperature (Tmin). **b**, Boxplot of averaged number of days with daily maximum temperature over 28 °C (Tmax28+), daily maximum temperature over 32 °C (Tmax32+), daily minimum temperature less than -10 °C (Tmin10-), and daily minimum temperature less than -15 °C (Tmin15-) for each month. Boxes in **a** and **b** show the median, an upper and lower hinge corresponding to the 25th and 75th percentiles of the distribution (first and third quartiles) and the whiskers, which show data dispersion up to 1.5 times the inter-quantile range; filled black circles are outliers.

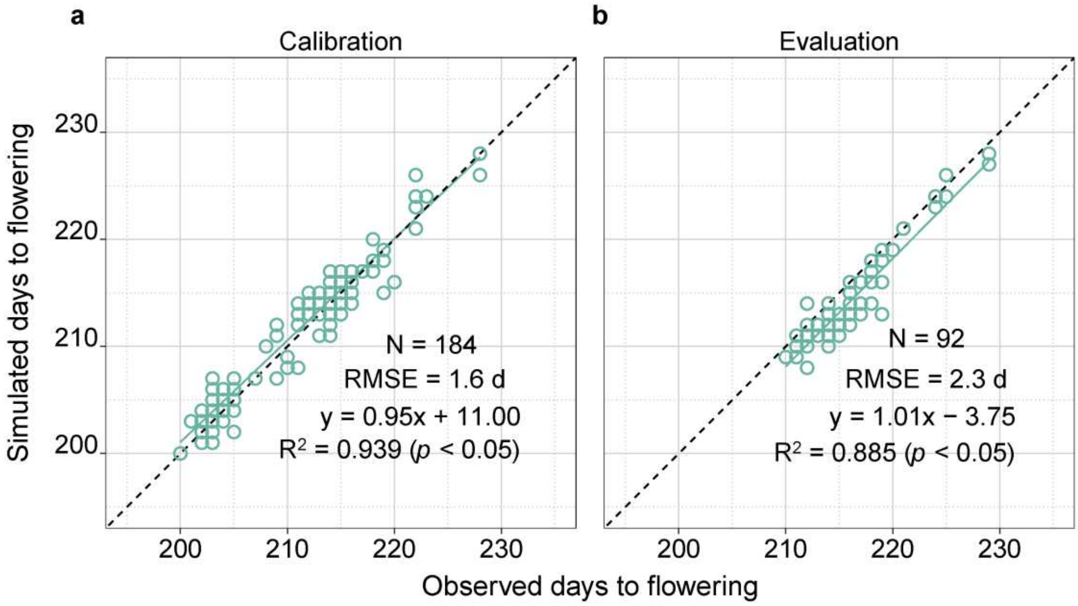


**Figure 5. Calibration and evaluation of the MLG-based model for modeling wheat-flowering-date**. **a**, Comparison of observed and simulated flowering dates for the calibration datasets using the MLG-based model. **b**, Comparison of observed and simulated flowering dates for the evaluation datasets using the MLG-based model (1:1, dashed line). The trial was conducted over three years in Beijing, China. Field test for calibrating and evaluating the MLG-based model was performed from 2016 to 2019 at the Beijing Shunyi Experimental Base (40°15′N, 116°55′E) of the Institute of Environment and Sustainable Development in Agriculture, Chinese Academy of Agricultural Sciences. Calibration datasets (2016-2017 and 2017-2018 growing seasons); Evaluation datasets (2018-2019 growing season).

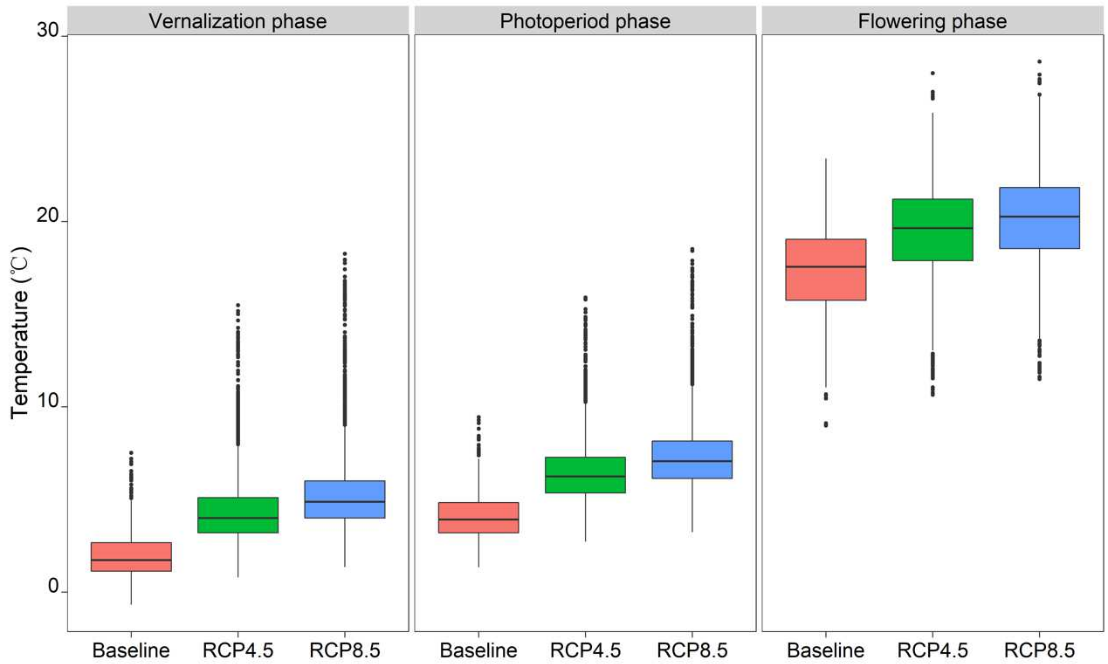


**Figure 6. Variation in air temperature for vernalization phase (emergence to floral initiation), photoperiod phase (emergence to start of flowering), and flowering phase (heading to start of flowering) under baseline (1981–2010), RCP4.5 and RCP8.5 projected climates (2036–2065) of the 16 locations of the Northern China Winter Wheat Region (NCWWR)**. Boxplot of averaged temperature (Tavg). Boxes show the median, an upper and lower hinge corresponding to the 25$^{th}$ and 75$^{th}$ percentiles of the distribution (first and third quartiles) and the whiskers, which show data dispersion up to 1.5 times the inter-quantile range; filled black circles are outliers. The phenological dates including emergence, floral initiation and start of flowering were obtained from a dataset of wheat phenology collected from agro-meteorological stations in China.

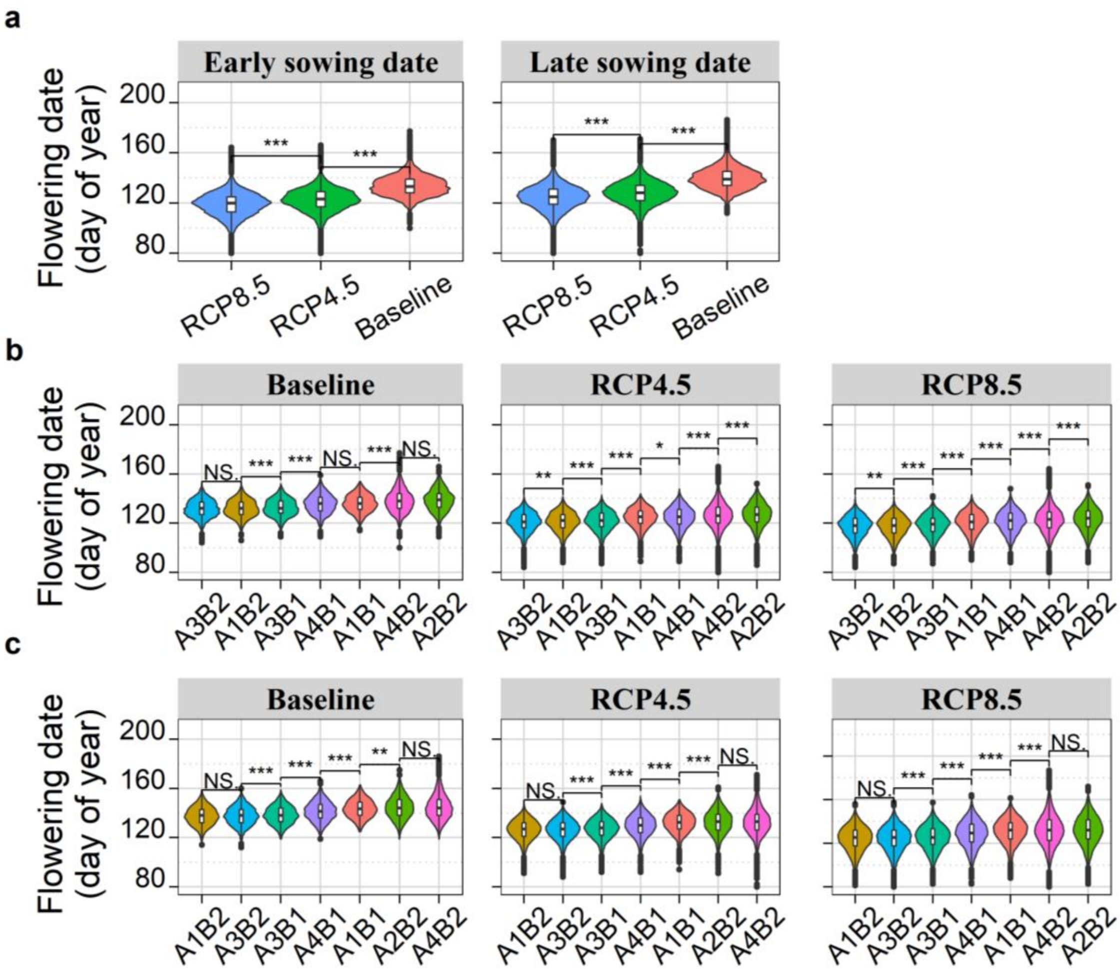


**Figure 7. Violin plots showing the distribution of the predicted wheat-flowering-date across the 16 locations in the Northern China Winter Wheat Region (NCWWR) using starting and ending sowing dates under baseline and RCP4.5 and RCP8.5 projected climates (multi-climate model ensemble), respectively, for different multi-locus genotypes (MLGs). a**, All MLGs, early sowing date, late sowing date. **b**, Early sowing date, baseline climate, RCP4.5 climate and, RCP8.5 climate. **c**, Late sowing date, baseline climate, RCP4.5 climate and, RCP8.5 climate. The photoperiod and vernalization alleles were combined in haplotypes in which A1 (*Ppd-A1a*+*Ppd-D1a*), A2 (*Ppd-A1a*+*Ppd-D1b*), A3 (*Ppd-A1b*+*Ppd-D1a*), and A4 (*Ppd-A1b*+*Ppd-D1b*) represent different photoperiod alleles, while B1 (*Vrn-D1*) and B2 (*vrn-D1*) represent different vernalization alleles. The early sowing dates were set to a range between September 21 and September 29, and the late sowing date was set to October 21. In **a**, **b** and **c**, the central mark is the median, lower (Q1) and upper (Q3) quartiles and the whiskers, which show data dispersion up to 1.5 times the inter-quantile range; filled black circles are outliers. Asterisks indicate statistically significant differences (*$p < 0.05$; ** $p < 0.01$; *** $p < 0.001$) or not significant (NS) ($p > 0.05$) based on the two-sided t-tests.

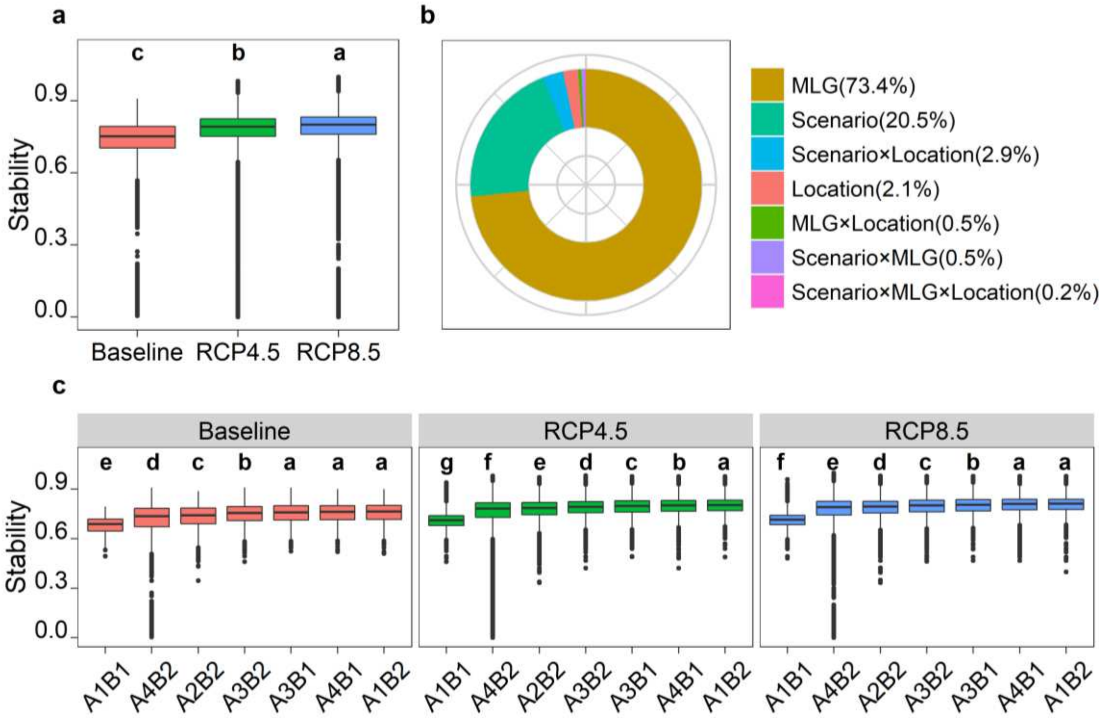


**Figure 8. The effect of climate change, multi-locus genotype (MLG), and location on the stability of the wheat-flowering-date across the 16 locations in the Northern China Winter Wheat Region (NCWWR). a**, Predicted stability of the wheat-flowering-date under baseline and RCP4.5 and RCP8.5 projected climates, respectively. **b**, Fraction of variance in the stability of the wheat-flowering-date according to MLG, temperature scenario, location, and the corresponding two- and three-way interactions for predicting flowering date stability. **c**, Predicted stability of the wheat-flowering-date for different MLGs under baseline and RCP4.5 and RCP8.5 projected climates, respectively (higher number indicates more stable). The photoperiod and vernalization alleles were combined in haplotypes in which A1 (*Ppd-A1a*+*Ppd-D1a*), A2 (*Ppd-A1a*+*Ppd-D1b*), A3 (P*pd-A1b*+*Ppd-D1a*), and A4 (*Ppd-A1b*+*Ppd-D1b*) represent different photoperiod alleles, while B1 (*Vrn-D1*) and B2 (*vrn-D1*) represent different vernalization alleles. In **a** and **c**, the central mark is the median, lower (Q1) and upper (Q3) quartiles and the whiskers, which show data dispersion up to 1.5 times the inter-quantile range; filled black circles are outliers, treatments (MLGs) sharing a letter do not significantly differ (Tukey-adjusted LSMeans comparisons; $p < 0.05$).

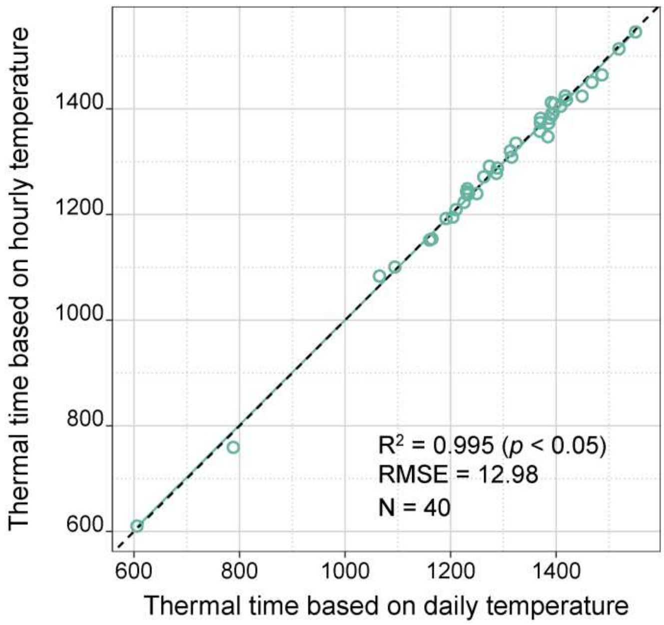


**Figure 9. Comparison of thermal time from 1 October (sowing date) to 1 May (flowering date) calculated by APSIM-Wheat-M using daily and hourly temperature (1:1, dashed line), respectively, from 1981 to 2020 in** Beijing Shunyi Experimental Base (40°15′N, 116°55′E) of the Institute of Environment and Sustainable Development in Agriculture, Chinese Academy of Agricultural Sciences. Field test for calibrating and evaluating the APSIM-Wheat-M model was performed from 2016 to 2019 at this site. Calibration datasets (2016-2017 and 2017-2018 growing seasons); Evaluation datasets (2018-2019 growing season).